

Characteristics and classification evaluation of tight sandstone reservoirs in the Shuixigou Group of the Taibei Sag, Turpan-Hami Basin

Qu XIYU¹*, Yang YUE², Zang CHUNYAN³, Yan ZHEN⁴ and Marcin RABE⁵

Authors' affiliations and addresses:

¹ China University of Petroleum (East China), Qingdao 266580, Shandong, China
e-mail: quxiyu@upc.edu.cn

² School of Geosciences, China University of Petroleum (East China), Qingdao 266580, Shandong, China
e-mail: 1901253265@qq.com

³ CNOOC Offshore Oil Development Engineering Technology Co., Ltd., Tianjin 300450, China
e-mail: 398415231@qq.com

⁴ Gudao Oil Production Plant, Sinopec Shengli Oilfield Company, Dongying 257231, China
e-mail: 2602681398@qq.com

⁵ Institute Management, University of Szczecin, Szczecin, Poland
e-mail: marcin.rabe@wzieu.pl

***Correspondence:**

Qu Xiyu, China University of Petroleum (East China), Qingdao 266580, Shandong, China
Tel.: 18669841029
e-mail: quxiyu@upc.edu.cn

Funding information:

National Science and Technology Major Project on New Oil and Gas Exploration and Development (2025ZD1400404 and 2025ZD1402802); The Natural Science Foundation of Shandong Province (ZR2024MD078).

How to cite this article:

Xiyu, Q., Yue, Y., Chunyan, Z., Zhen, Y. and Rabe, M. (2025). Characteristics and classification evaluation of tight sandstone reservoirs in the Shuixigou Group of the Taibei Sag, Turpan-Hami Basin, *Acta Montanistica Slovaca*, Volume 30 (3), 622-636

DOI:

<https://doi.org/10.46544/AMS.v30i3.06>

Abstract

This study focuses on the Xishanyao and Sangonghe Formation tight sandstone reservoirs within the Shuixigou Group of the Taibei Sag in the Turpan-Hami Basin. Using thin section identification, scanning electron microscopy (SEM) observations, and high-pressure mercury injection (HPMI) tests, we systematically analyzed the petrophysical properties, reservoir space features, and diagenetic characteristics of these tight sandstone reservoirs. The interrelationships between reservoir parameters and petrophysical indicators were thoroughly investigated, finally establishing a comprehensive evaluation system tailored to tight sandstone reservoirs in this area. The results indicate that the tight sandstone in the study area is primarily lithic sandstone, characterized by relatively poor particle sorting and rounded grains. The reservoir porosity and permeability are both low, and the storage space is primarily composed of secondary pores. The study area has undergone diagenetic processes, including compaction, cementation, dissolution, and replacement. Among these, compaction has had the most destructive impact on reservoir properties, cementation has had a dual effect, while dissolution has improved reservoir quality. Porosity is positively correlated with sandstone grain size, permeability, median radius, average throat radius, and maximum mercury saturation, but negatively correlated with cement content, bound water saturation, and displacement pressure. Based on mercury injection curves, the reservoirs can be classified into four types according to porosity intervals. Using the above evaluation indicators, a classification and evaluation standard for tight sandstone reservoirs in the Shuixigou Group of the Taibei Sag is established.

Keywords

Taibei Sag; Shuixigou Group; Tight sandstone reservoir; Main control factors; Reservoir Evaluation



© 2025 by the authors. Submitted for possible open access publication under the terms and conditions of the Creative Commons Attribution (CC BY) license (<http://creativecommons.org/licenses/by/4.0/>).

Introduction

Tight sandstone oil and gas exploration in China has become increasingly active. Two major tight sandstone gas-producing regions have already been identified in the Ordos Basin and the Sichuan Basin. In addition, five other basins show strong potential: the Turpan-Hami Basin, the southern margin of the Junggar Basin, the Tarim Basin, the Bohai Bay Rim, and the Songliao Basin (Li et al., 2015). As China's economy increasingly relies on oil and gas resources and the difficulty of exploration continues to rise (Zhou et al., 2021), tight sandstone oil and gas resources have emerged as both a key unconventional replacement resource (Jia et al., 2022) and an important target for expanding conventional natural gas reserves in the future (Dai et al., 2024). Many countries worldwide are actively engaged in the exploration and development of tight oil and gas resources. Currently, tight sandstone gas reserves that can be extracted using existing exploration and development technologies rank first among unconventional gases. China's tight sandstone gas reservoirs are widely distributed and diverse in type. However, due to the typically low porosity and permeability of tight sandstone reservoirs, as well as intense diagenesis (Yu et al., 2024), their complex reservoir formation mechanisms pose significant challenges to oil and gas exploration and development (Dai et al., 2024; Li & Zhu, 2020).

In recent years, significant progress has been made in the exploration of deep formations in the Turpan-Hami Basin, which has now become a promising area for onshore tight oil and gas exploration in China (Zhi et al., 2024). Guided by coal-derived hydrocarbon theory, more than 20 oil and gas fields have been successfully discovered and proven, with cumulative oil and gas geological reserves reaching 5.4×10^8 t. In recent years, many experts and scholars have conducted in-depth research on the Jurassic tight sandstone oil and gas deposits in the Turpan-Hami Basin, concluding that the basin possesses abundant tight sandstone oil and gas resources (Hao et al., 2025). Previous studies on the Shuixigou Group in the Taibei Sag of the Turpan-Hami Basin have focused on sedimentary systems, reservoir diagenesis, and hydrocarbon accumulation (Si et al., 2014; Ni et al., 2022; Ma, 2024; Wang et al., 2016), preliminarily establishing reservoir evaluation indicators primarily based on macroscopic parameters such as porosity, permeability, sandstone grain size, and sedimentary facies. While these macroscopic indicators are somewhat applicable for classifying and characterizing conventional sandstone reservoirs, they fall short in accurately evaluating the complex microscopic pore structure characteristics of tight sandstone reservoirs and their impact on reservoir flow capacity.

Therefore, it is essential to scientifically select reservoir evaluation parameters, optimize evaluation methods suitable for the study area, and achieve reservoir classification and evaluation. Accordingly, this study focuses on the Xishanyao and Sangonghe Formations within the coal-bearing strata of the Shuixigou Group in the Taibei Sag of the Turpan-Hami Basin. By integrating methods such as cast thin section analysis, high-pressure mercury injection, and scanning electron microscopy, the basic petrological characteristics of the target reservoir formations in the study area are clarified. Building on previous macroscopic evaluation indicators, key microscopic pore structure parameters are supplemented and integrated to provide a comprehensive understanding. The correlations between porosity and various reservoir parameters are established to determine the influence of different reservoir parameters on reservoir properties, identify the main parameters for practical reservoir evaluation, and select significant reservoir parameters to establish an evaluation standard for tight sandstone reservoirs.

Regional Geological Overview

The Turpan-Hami Basin, one of Xinjiang's three major oil and gas basins, extends east–west across eastern Xinjiang, separated by mountain ranges and flanked by the Tarim and Junggar basins to its north and south, respectively (Dong, 2023). The basin extends approximately 660 km east–west and 60–130 km north–south, covering an area of approximately 5.35×10^4 km 2 . From west to east, it can be divided into three primary structural units: the Turpan Sag, the Liaodun Uplift, and the Hami Sag (He et al., 2022). The Taibei Sag in the study area constitutes the largest secondary structural unit within the Turpan-Hami Basin. It serves as the primary sedimentary sag of the Turpan Sag, covering an area of approximately 1.09×10^4 km 2 (Li et al., 2025). From west to east, it is further subdivided into three negative structural units: the Shengbei Sub-Sag, the Qiudong Sub-Sag, and the Xiaocaohu Sub-Sag (Hao et al., 2021)(Fig. 1a).

The sedimentary sequence of the Taibei Sag is primarily composed of clastic rocks interbedded with volcanic rocks. Jurassic strata are widely distributed and well-developed throughout the basin, exhibiting favorable reservoir conditions and potential as source rocks (Zhang et al., 2019). The Lower Jurassic Badaowan and Sangonghe Formations, together with the Middle Jurassic Xishanyao Formation, constitute the Shuixigou Group. The Sangonghe Formation (J_{1s}) and Xishanyao Formation (J_{2x}) are the target formations of this study (Fig. 1b), primarily formed in environments such as shallow coastal lakes, rivers, swamps, and braided river deltas (Ni et al., 2019). The Sangonghe Formation exhibits typical sandstone-mudstone interbedding, with relatively well-developed sandstones topped by a series of gray mudstones (Zhou, 2020). The Xishanyao Formation comprises a coal-bearing clastic sequence, with the upper sandstone section serving as a key

hydrocarbon reservoir in the area. In contrast, the lower section hosts an important coal-bearing hydrocarbon source rock.

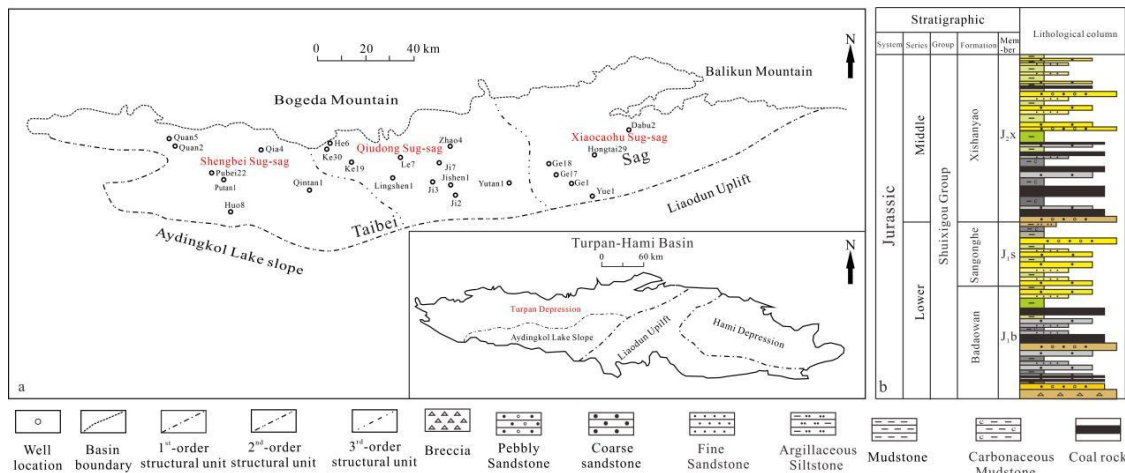


Fig. 1. Tectonic unit division of the Taihei Sag in the Turpan-Hami Basin (a) and integrated stratigraphical column of the Shuixigou Group (b) (according to Ref. (Xiao et al., 2024))

Characteristics of the Tight Sandstone Reservoirs

Reservoir Lithological Characteristics

Sandstone types and structural characteristics of tight sandstone intervals were identified through microscopic analysis of reservoir samples and statistical study of 67 cast thin sections from 30 wells across three sags and two strata in the Turpan-Hami Basin. The rock types in the target formations of the study area are predominantly clastic sandstone, followed by feldspar clastic sandstone (Fig. 2). In terms of grain size, the reservoir rocks are predominantly medium- to coarse-grained sandstones and fine sandstones, with minor gravel and siltstone components. They exhibit moderate matrix content, strong compaction, diverse clast and cement types, and low compositional and structural maturity (Fig. 3a, b). Structurally, reservoirs in the Taihei Basin exhibit pronounced proximal rapid deposition characteristics. Clastic grain sorting is generally poor, with roundness predominantly subangular to subrounded, and some subangular grains present. Weathering and alteration are moderate, with inter-grain contacts predominantly linear, supplemented by point and convex-concave contacts. Grain-type support structures dominate (Fig. 3a, b), indicating the target sandstone in the study area underwent intense compaction. From the perspective of framework grain characteristics, the study area exhibits diverse clast assemblages, predominantly composed of igneous and metamorphic clasts, with sedimentary clasts relatively scarce within the detrital fraction. Among these, igneous clasts are primarily granitic clasts (Fig. 3c) and acidic volcanic clasts (Fig. 3d); metamorphic clasts are mainly metamorphic quartzite clasts (Fig. 3e) and chert clasts (Fig. 3f).

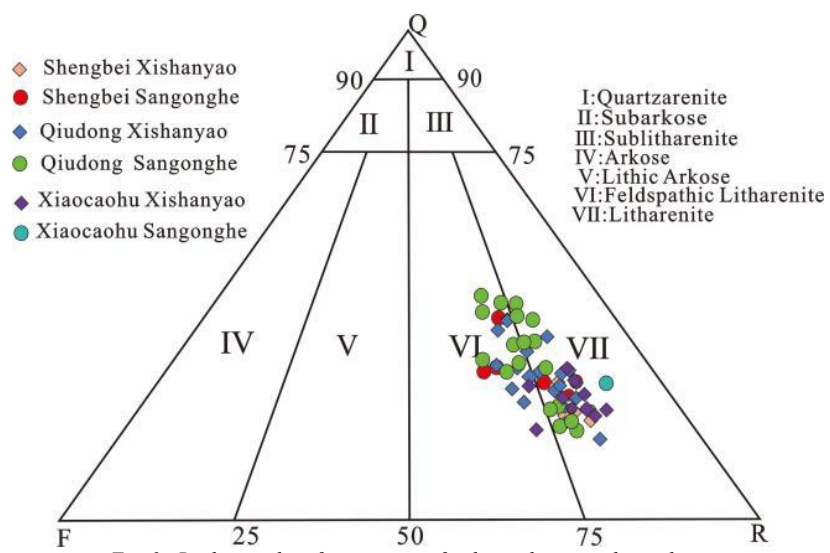
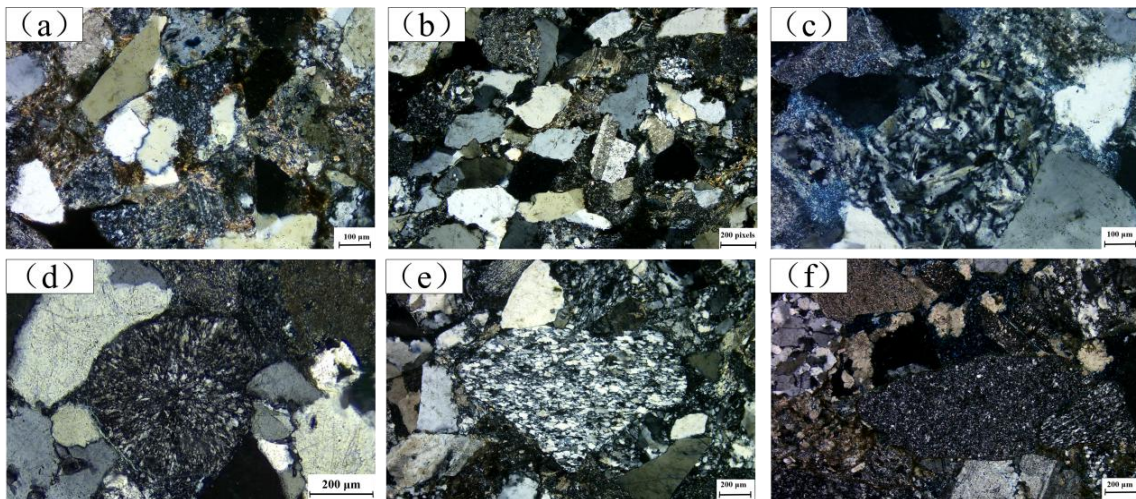


Fig. 2. Rock type classification map of tight sandstone in the study area



Note: a: Shengbei Sub-sag, Qintan 1 Well, 5083.82 m, feldspar-rich sandstone (+); b: Qiudong Sub-sag, He 5 Well, 2059.22 m, feldspar elastic sandstone (+); c: Qiudong Sub-sag, Ji 702 Well, 5349.3 m, granite clasts (+); d: Qiudong Sub-sag, Ji Shen 1 Well, 3779.17 m, acidic volcanic rock cuttings (+); e: Shengbei Sub-sag, Hongnan 4 Well, 3582.05 m, metamorphic quartzite cuttings (+); f: Xiaocaohu Sub-sag, Ge 17 Well, 2931.7 m, flint cuttings (+).

Fig. 3. Petrologic and lithic fragment types characterization of tight sandstone reservoirs in the study area

Reservoir Physical Properties

The tight sandstone reservoirs in the Shuixigou Group of the Taibei Sag, Turpan-Hami Basin, exhibit relatively low porosity and permeability values (Zhang et al., 2011; Liu et al., 2014). Analysis of 306 sets of physical property data collected from 31 tested wells reveals a wide range of distributions for porosity and permeability in the study area. However, most porosity values fall below 10%, accounting for 93.8% of all data. The majority of porosity values are concentrated between 3% and 8%, representing 79% of all data. The 5%–6% porosity range exhibits the highest proportion at 19.61% (Fig. 4a). Permeability values predominantly range between 0.01 and 1 mD, with values below 0.3 mD accounting for the majority at 69.28% of all data. The 0.1–0.2 mD permeability range has the highest proportion at 27.45% (Fig. 4b). Furthermore, porosity and permeability exhibit a significant positive correlation, meaning higher porosity corresponds to increased permeability (Fig. 5). Specifically, samples with a porosity of $\leq 3.5\%$ generally have permeability below 0.2 mD; samples with a porosity between 3.6% and 6% are primarily concentrated between 0.05 and 0.5 mD; samples with a porosity between 6.1% and 10% mainly exhibit permeability values between 0.1 and 1 mD; and samples with a porosity of $> 10\%$ typically exhibit permeability values exceeding 0.5 mD.

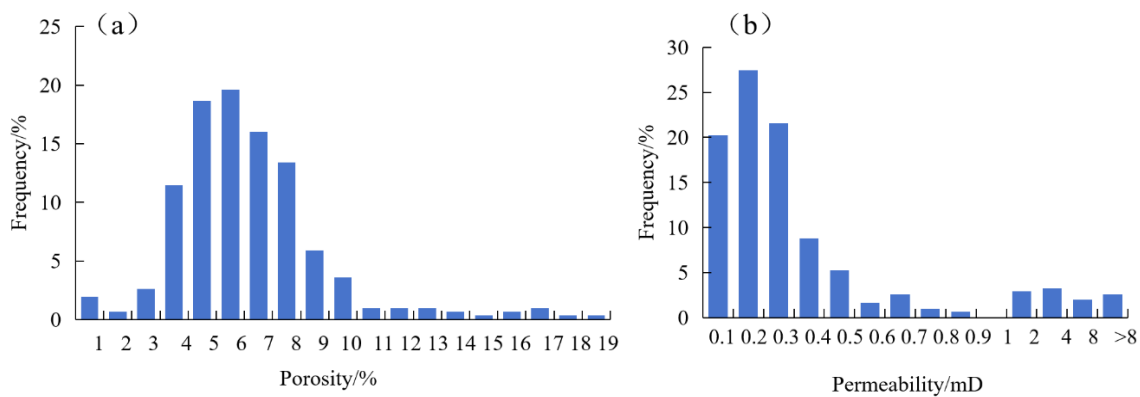


Fig. 4. Frequency distribution histograms of porosity (a) and permeability (b) in tight sandstone reservoirs of the study area

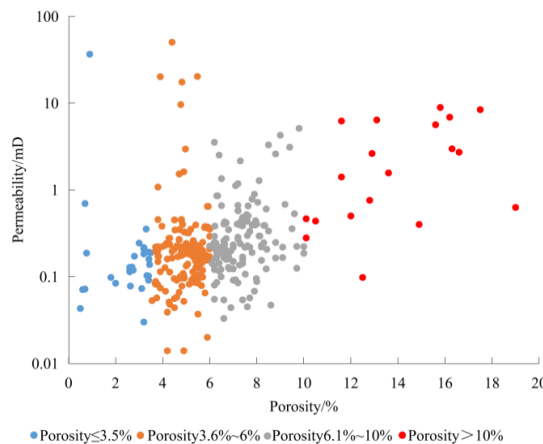
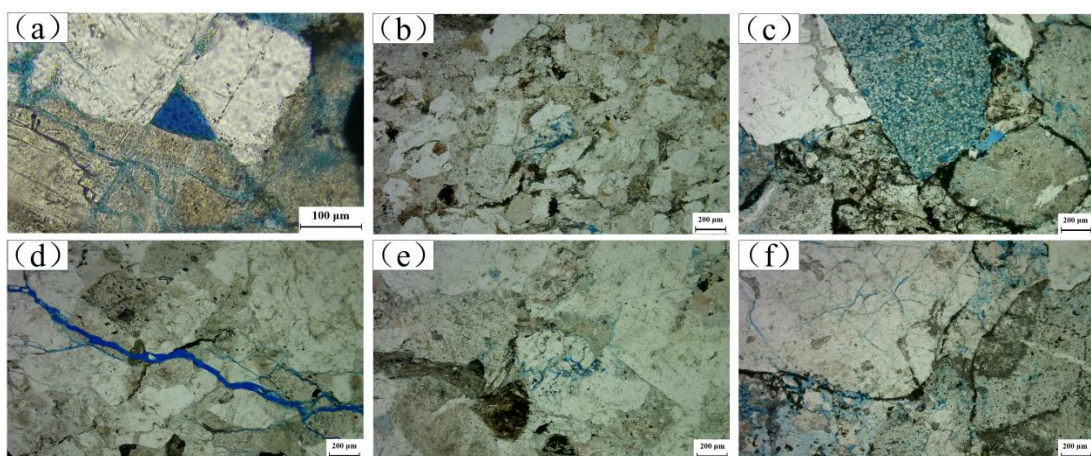


Fig. 5. Relationship Between porosity and permeability in Tight Sandstone Reservoirs of the Study Area

Reservoir Storage Space Types

The Xishanyao and Sangonghe Formations in the Taihei Sag of the Turpan-Hami Basin are governed by diverse tectonic settings, sedimentary environments, and complex diagenetic processes, resulting in intricate and varied reservoir storage space types and combinations (Hao et al., 2020). Thin section observations reveal that reservoir storage space types in the target formation of the study area can be classified into three categories based on genesis: primary, secondary porosity, and fractures.

Primary porosity in the study area is limited, consisting mainly of residual intergranular pores. Most were destroyed during diagenesis, leaving native primary pores almost unobservable. Under the microscope, they appear as well-defined triangular or polygonal grain-boundary pores (Fig. 6a), commonly filled with carbonate cement or clay minerals. Secondary pores exhibit diverse development in the study area, including intergranular dissolution pores and intragranular dissolution pores. Intragranular dissolution pores dominate, predominantly feldspar dissolution pores (Fig. 6b) and various clast dissolution pores (Fig. 6c). Fractures exhibit irregularly curved shapes (Fig. 6d, e, f), with grain-adjacent fractures—also termed grain fractures—developing along particle edges and exhibiting weak connectivity. The development of such fractures correlates with particle roundness (Cheng, 2021). Microfractures exhibit trans-grain characteristics. Although their contribution to total pore volume is relatively limited, they serve as critical filtration pathways within reservoirs, significantly enhancing connectivity between pores and playing a pivotal role in improving reservoir permeability (Ban, 2022).



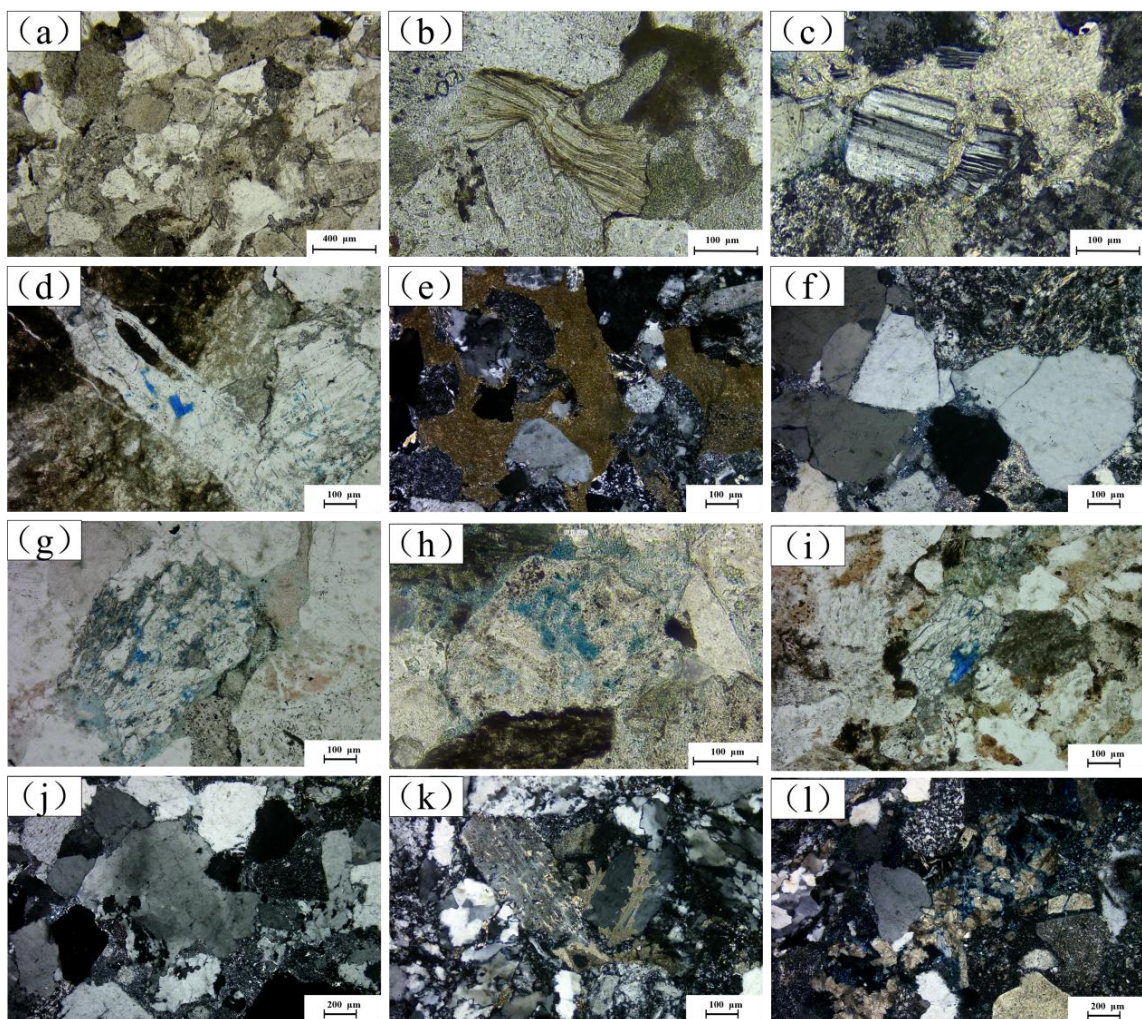
Note: a: Shengbei Sub-sag, Quan 2 Well, 2690.4 m, residual intergranular voids (-) b: Shengbei Sub-sag, Qintan 1 Well, 5082.24 m, feldspar dissolution voids (-) c: Xiaocaohu Sub-sag, Ge 17 Well, 2931.5 m, cuttings dissolution voids (-) d: Qiudong Sub-sag, Ji 702 Well, 5351.14 m, Fracture (-); e: Qiudong Sub-sag, Ji 702 Well, 5350.2 m, Microfracture in feldspar (-); f: Xiaocaohu Sub-sag, Ge 17 Well, 2931.8 m, Microfracture in quartz (-).

Fig. 6. Space types within the tight sandstone reservoirs of the study area.

Diagenetic Characteristics of Reservoirs

Using thin sections and scanning electron microscope analysis of over 280 tight sandstone casts from the study area, this study systematically examines the diagenetic characteristics of Shuixigou Group sandstone reservoirs in the Taibei Sag, Turpan-Hami Basin. It is concluded that the reservoirs in this area are primarily influenced by four diagenetic processes: compaction, cementation, dissolution, and replacement. Compaction is pronounced in the study area, with closely packed grains. Cementation and replacement are widespread, while dissolution is generally weak, dominated by acid dissolution, with some quartz exhibiting alkaline dissolution.

Due to significant burial depth, compaction is the predominant diagenetic process in the Shuixigou Group of the Taibei Sag, Turpan-Hami Basin. It causes the most destructive effects on reservoir properties and is one of the reasons for the widespread tightness of target reservoirs. For the target formations in the study area, intense compaction resulted in predominantly line-contact grain interactions (Fig. 7a), with minimal point-contact and localized convex-concave contacts. Plastic grains, such as mica, phyllite, schist, and slate, as well as glass fragments, underwent bending deformation under stratigraphic pressure (Fig. 7b), filling primary pore spaces and significantly reducing porosity and permeability (Li et al., 2024). Meanwhile, brittle grains like feldspar readily fracture under tectonic pressure (Fig. 7c). The resulting fractures typically extend along cleavage planes and are often filled with matrix material and autogenous siliceous bands.



Note: a: Qiudong Sub-sag, Ji 7 Well, 5334.2 m, linear contact between grains (-); b: XiaoCaohu Sub-sag, Ge 1 Well, 1360.97 m, compacted deformation of biotite (-); c: Qiudong Sub-sag, Ling Shen1 Well, 4181.26 m, compacted faulting of feldspar (+); d: Qiudong Sub-sag, Ji 702 Well, 5349 m, banded dolomite cementation (-); e: XiaoCaohu Sub-sag, Ge 17 Well, 2929.5 m, clay mineral cementation (+); f: Qiudong Sub-sag, Ji 702 Well, 5349.8 m, secondary quartz enlargement (+); g: Qiudong Sub-sag, Ji 702 Well, 5349.07 m, feldspar grain dissolution (-); h: XiaoCaohu Sub-sag, Hongtai 306 Well, 2858.43 m, acidic volcanic clast dissolution (-); i: Shengbei Sub-sag, Qin Tan 1 Well, 5082.24 m, calcareous cement dissolution (-); j: Qiudong Sub-sag, Ji 702 Well, 5350.3 m, quartz grain boundaries eroded into bay-like shapes (+); k: Shengbei Sub-sag, Hongnan 4 Well, 3582.05 m, feldspar sericitization (+); l: XiaoCaohu Sub-sag, Ge 17 Well, 2930.85 m, dolomite replacement of feldspar and clasts (+)

Fig. 7. Types of diagenesis in the tight sandstone reservoirs of the study area

The study area exhibits diverse types of cementation, including calcareous, siliceous, and clay mineral cementation. Cementation both reduces original pore space and strengthens the rock against compaction, thereby limiting further pore loss. The study area underwent multiple cycles of alternating acid and alkaline fluid evolution, resulting in complex cementation patterns. Microscopic thin section observations reveal that calcareous cementation, predominantly dolomite (Fig. 7d), and autogenous clay mineral cementation (Fig. 7e) dominate the study area, with siliceous cementation also developing in some sections (Fig. 7f). Siliceous cementation is generally characterized by secondary quartz enlargement and chert cementation.

Secondary porosity formed by dissolution is a key factor in enhancing reservoir porosity (Zhou et al., 2023), as it alters reservoir porosity and permeability, thereby improving reservoir properties. The target formation in the study area is a typical coal-bearing stratum characterized by acidic dissolution. Thin section observations reveal numerous intragranular dissolution pores in feldspar and rock fragment grains (Fig. 7g, h), providing favorable reservoir space for hydrocarbon accumulation. Significant cement dissolution is also present, as seen in the dissolution of carbonate cement (Fig. 7i), whereas quartz grain dissolution is relatively uncommon (Fig. 7j).

Replacement is widespread in the study area. Common types include chiefly the sericitization of feldspar (Fig. 7k) and the replacement of feldspar or lithic fragments by carbonate minerals (Fig. 7l). The products of replacement fill secondary dissolution pores, indicating that the replacement occurred after the dissolution events.

Classification Evaluation Criteria for the Tight Sandstone Reservoirs

Selection of Key Parameters

Petrological and Sedimentological Characteristics

(1) Rock Type

Rock types in the study area were classified by statistically analyzing the proportions of quartz, feldspar, and lithic fragments in thin sections of each sample. These data were then plotted on a clastic lithology classification triangle (Fig. 8). Classification by porosity range revealed that samples with a porosity of $> 10\%$ were dominated by clastic sandstone; samples with a porosity between 6% and 10% were dominated by clastic sandstone, followed by feldspar clastic sandstone; samples with a porosity between 3.5% and 6% primarily exhibited clastic sandstone lithology; and samples with a porosity of $\leq 3.5\%$ were also dominated by clastic sandstone. Within sandstone reservoirs, clastic grains are plastic particles that exhibit the poorest resistance to compaction, which is negatively correlated with reservoir properties. Quartz, as a rigid mineral, enhances rock resistance to compaction while preserving primary intergranular pores and serving as the material basis for secondary dissolution pore formation. Sediment porosity positively correlates with quartz content (Wang et al., 2023). Feldspar clasts exhibit poor stability and are prone to dissolution, with their content influencing the development of dissolution pores (Zhang, 2020). Research findings indicate that porosity is weakly influenced by rock type, with clastic sandstone being the predominant type, regardless of the porosity level. This may relate to the acidic diagenetic environment of the target formation in the study area and the widespread deep burial of coal-bearing strata. Under deep burial conditions, quartz grains readily undergo crushing and dissolution, forming microfractures. In contrast, feldspar undergoes dissolution due to compaction and dissolution, thereby increasing reservoir space and improving reservoir permeability. However, in the Shuixigou Group reservoirs of the Taibei Sag in the Turpan-Hami Basin, the quartz and feldspar contents are relatively low, exerting a minimal influence on reservoir properties, and the rock type does not demonstrate a significant controlling effect (Zhou, 2020).

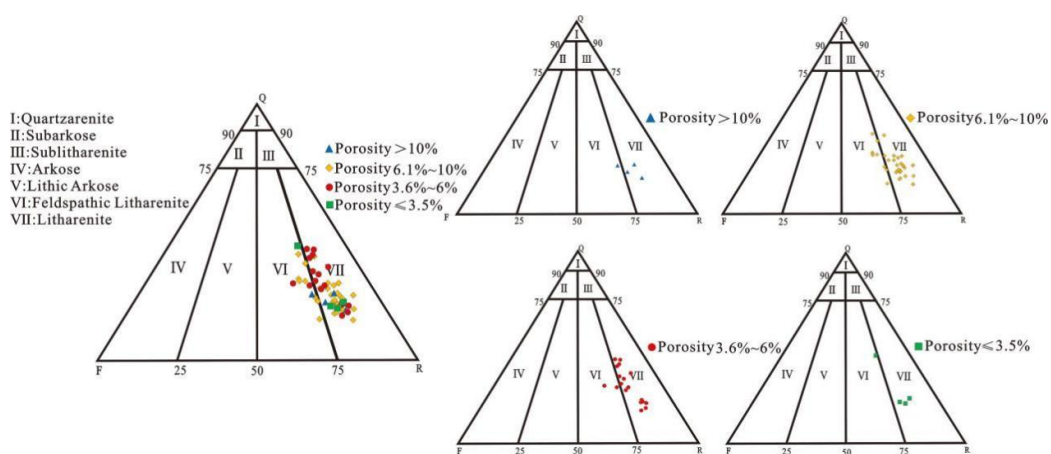


Fig. 8. Petrographic classification of tight sandstones in the study area

(2) Sandstone Grain Size

Based on measured sandstone porosity, four intervals were defined, ranging from the highest to the lowest porosity. The sandstone grain size distribution within each porosity interval was statistically analyzed, yielding frequency distribution histograms for different grain sizes across varying porosity ranges (Fig. 9). The histograms reveal that fine sandstone exhibits the highest distribution frequency in all porosity intervals, indicating that fine sandstone dominates the grain size distribution within the study area. Excluding the most abundant fine sandstone, samples with a porosity of $\leq 3.5\%$ are predominantly medium sandstone; those with a porosity of 3.6%–6% are mainly medium sandstone with gravel; samples with a porosity of 6.1%–10% are primarily coarse sandstone; and samples with a porosity of $> 10\%$ are also predominantly coarse sandstone, with a higher proportion relative to the 6%–10% porosity range. The grain size-porosity relationship diagram indicates that coarser sandstones (for instance, coarse sandstone and conglomerate) exhibit relatively higher porosity. This arises because coarse-grained sandstones typically form in strong hydrodynamic environments, where sedimentation significantly reduces matrix content. This not only creates primary intergranular pores with larger apertures and coarser throats but also facilitates subsequent dissolution processes. Conversely, fine-grained sandstones exhibit weaker resistance to compaction, making them more susceptible to pore structure destruction during burial. This results in a significant decline in reservoir properties (Yang, 2021).

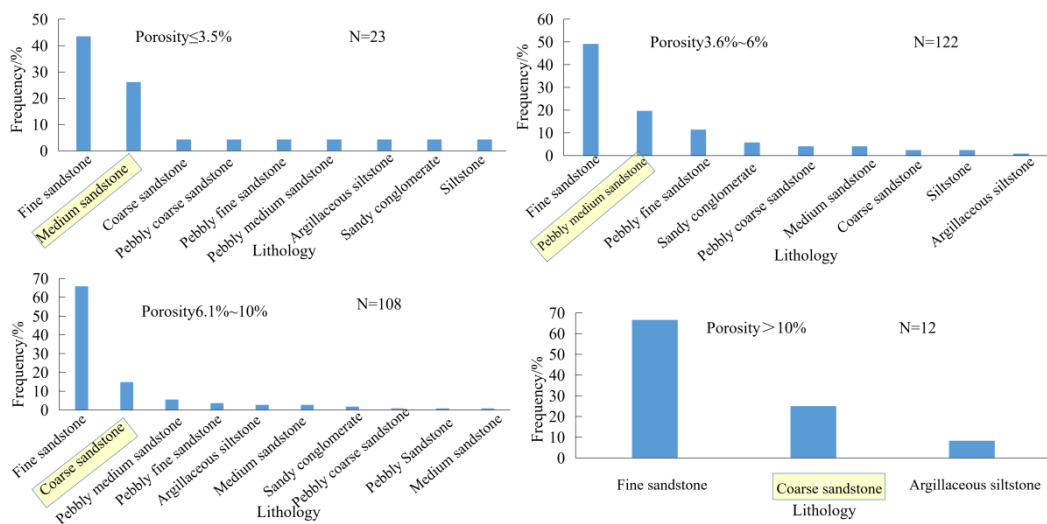


Fig. 9. Frequency diagram of the distribution of sandstones with different grain sizes in the study area

(3) Sand Body Thickness and Sedimentary Microfacies

Sand body thickness exhibits a positive correlation with physical properties. This is primarily because thicker sandstone layers contain more erodible grains, facilitating the formation of numerous secondary dissolution pores. Later-stage cementation typically fills the top and bottom of the sandstone, effectively preserving secondary porosity within thick sandstone layers (Guo, 2023). Sedimentary facies primarily influence reservoir properties by controlling the grain size and sorting of sandstone. In shallow-water braided delta foreshore environments, subaqueous distributary channel microfacies sandstones are coarse-grained, well-sorted, and low in matrix content due to strong hydrodynamics. Their compaction resistance promotes primary porosity preservation and superior pore structures, creating favorable conditions for subsequent dissolution (Zhou, 2023). In contrast, sandstones deposited in shallow lacustrine environments exhibit finer grains and good sorting due to repeated modification by lake waves and currents; however, they generally form thinner sand bodies.

Cementation Characteristics

Statistical analysis of the relationship between cementation content and porosity reveals that samples with a porosity of $\leq 3.5\%$ generally exhibit cementation content exceeding 15%. Samples with a porosity between 3.6% and 6% predominantly have cementation content ranging from 4% to 18.5%. For samples with a porosity between 6.1% and 10%, cement content mostly ranges from 4.5% to 12.5%. For samples with a porosity of $> 10\%$, cement content is typically below 10% (Fig. 10). This indicates a significant negative correlation between porosity and cement content: samples with lower porosity typically exhibit higher cement content, while those with higher porosity show relatively lower cement content. This occurs because calcareous, siliceous, and clay mineral cements formed during cementation fill intergranular pores, significantly reducing adequate reservoir space and creating flow barriers that decrease permeability. Although early cementation can partially enhance rock resistance to compaction, its overall negative impact on porosity and permeability throughout the diagenetic

process is more pronounced. This often leads to irreversible deterioration of reservoir properties, with different cement types exerting varying effects on reservoir characteristics. Siliceous cementation (primarily manifested as secondary quartz enlargement) filling pores not only reduces pore space but also alters the reservoir's pore structure, diminishing fluid flow capacity and degrading reservoir permeability (Tang et al., 2015). Calcareous cementation (for instance, carbonate minerals such as calcite and dolomite) typically impairs reservoir permeability; higher concentrations are correlated with poorer reservoir properties. However, moderate amounts of calcite can generate secondary pores and microfractures through dissolution or fracturing, effectively increasing reservoir storage capacity and permeability (Liu et al., 2018). Clay mineral cementation (primarily chlorite) improves reservoir properties by enhancing rock resistance to compaction and inhibiting the secondary grain growth of quartz and other particles (Chen et al., 2016). Conversely, densely distributed or excessive chlorite can clog pores and disrupt connectivity (Ajdukiewicz & Larese, 2012). Furthermore, cementation can alter reservoir properties by influencing clay mineral content, thereby changing the pore size distribution. Pores smaller than 1 μm —including micropores, mesopores, and macropores—are collectively called nanopores. Statistical analysis of nanopore percentage, combined with X-ray diffraction testing of clay mineral content in samples, reveals a positive correlation between nanopore fraction and clay mineral content (Fig. 11). A high nanopore fraction may imply reduced macropores, but whether reservoir properties deteriorate depends on specific conditions. For reservoirs dominated by adsorbed gas (for instance, shale gas), nanopores may enhance adsorption and gas storage capacity, though permeability may decrease. Conversely, reservoirs requiring larger pores and throats to maintain permeability may be disadvantaged by a high nanopore fraction.

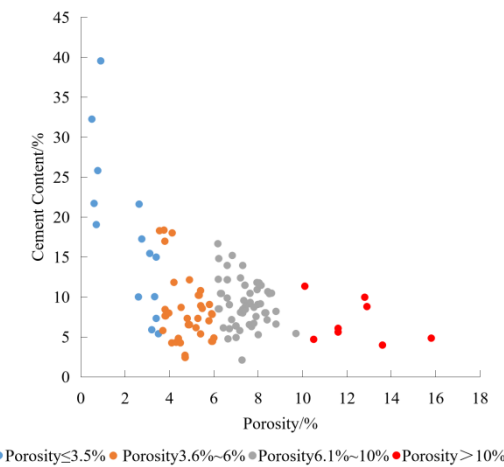


Fig. 10. Relationship Between Porosity and Cement Content in Tight Sandstone Reservoirs of the Study Area

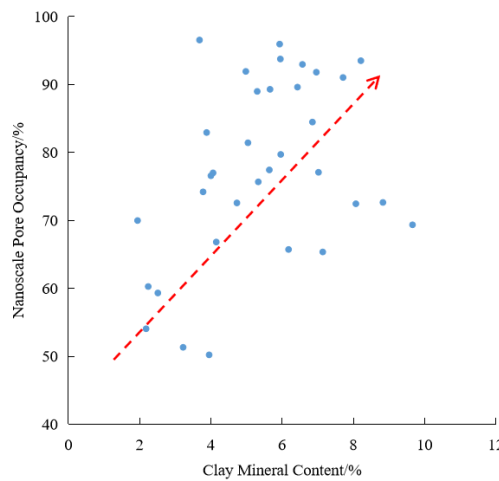


Fig. 11. Relationship between nanoscale pore occupancy and clay mineral content in Tight Sandstone Reservoirs of the Study Area

Nuclear Magnetic Parameters

Nuclear magnetic resonance (NMR) measurements of mobile fluid saturation effectively indicate reservoir fluid flow properties. As an integrated measure of reservoir quality, it is a key parameter for assessing the development potential of tight oil (Xu, 2019). Analysis of the relationship between NMR parameters and

porosity reveals that samples with a porosity of $\leq 3.5\%$ generally exhibit bound water saturation above 55%; samples with a porosity between 3.6% and 6% predominantly show bound water saturation between 45% and 55%; for samples with a porosity between 6.1% and 10%, bound water saturation is mainly distributed between 37% and 45%; for samples with a porosity $> 10\%$, bound water saturation is typically below 40% (Fig. 12). This indicates a clear negative correlation between bound water saturation and porosity, where lower porosity is associated with higher bound water saturation. This occurs because, as porosity decreases, the pore structure becomes more complex, leading to a significant increase in the proportion of fine throats within the reservoir, which in turn elevates bound water saturation (Wang et al., 2014). In contrast to bound water saturation, mobile fluid saturation increases significantly with increasing porosity. However, no clear regular relationship was observed between the characteristics of the sample's NMR T_2 spectrum curve and porosity.

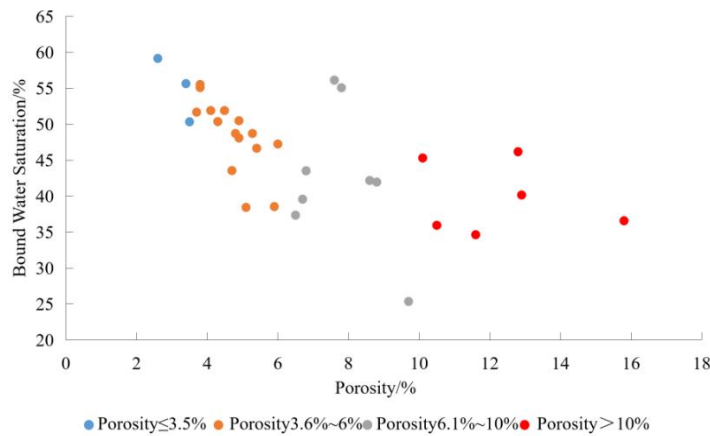


Fig. 12. Relationship between bound water saturation and porosity in Tight Sandstone Reservoirs of the Study Area

Pore Structure

Analysis of the relationship between mercury displacement parameters and porosity yields the following conclusions. Both the median radius and average throat radius exhibit a significant positive correlation with porosity. That is, as porosity increases, both the median radius and average throat radius show an increasing trend (Fig. 13a, b). Additionally, displacement pressure exhibits a negative correlation with porosity, while maximum mercury saturation shows a positive correlation. Specifically, higher porosity corresponds to lower displacement pressure and higher maximum mercury saturation (Fig. 13c, d). Mercury intrusion parameters exhibit distinct variations across different porosity ranges: for samples with a porosity of $\leq 3.5\%$, the median radius is $< 0.01 \mu\text{m}$, the average throat radius is $< 0.05 \mu\text{m}$, the displacement pressure exceeds 1.4 MPa, and the maximum mercury saturation remains below 50%. For samples with a porosity between 3.6% and 6%, the median pore radius ranges from 0.005 to $0.01 \mu\text{m}$, the average throat radius spans 0.05 to $0.25 \mu\text{m}$, the displacement pressure falls between 0.4 and 1.4 MPa, and the maximum mercury saturation reaches 50% to 70%. For samples with a porosity between 6.1% and 10%, the median pore radius ranges from 0.01 to $0.1 \mu\text{m}$, the average throat radius is between 0.1 and $0.4 \mu\text{m}$, the displacement pressure is 0.25 to 1.4 MPa, and the maximum mercury saturation reaches 57% to 83%. For samples with a porosity greater than 10%, the median pore radius exceeds $0.1 \mu\text{m}$, the average throat radius surpasses $0.4 \mu\text{m}$, the displacement pressure is below 0.7 MPa, and the maximum mercury saturation exceeds 70%.

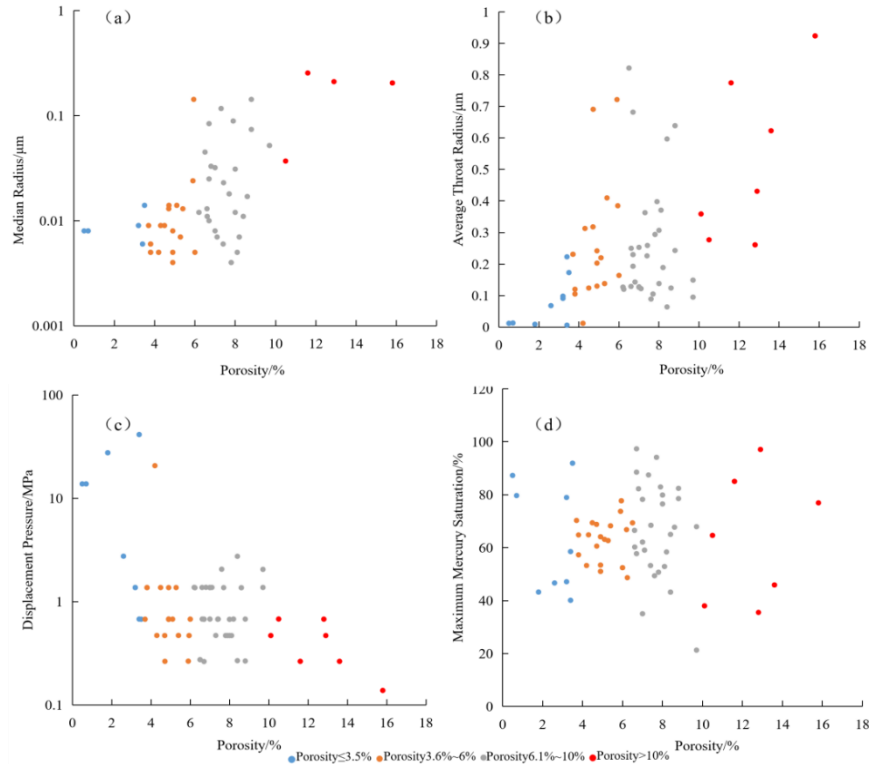


Fig. 13. Correlation analysis between porosity and mercury injection parameters in tight sandstone reservoirs of the Study Area(a) Relationship between Porosity and Median Radius(b) Relationship between Porosity and Average Throat Radius(c) Relationship between Porosity and Displacement Pressure(d), and Relationship between Porosity and Maximum Mercury Saturation

The mercury porosimetry curve morphology also exhibits distinct variations with changes in sample porosity (Fig.14). For samples with a porosity of $\leq 3.5\%$, the capillary pressure curve presents a narrow upward bulge pattern. Samples with a porosity between 3.6% and 6% exhibit wavy or short sloping curves. Samples with a porosity between 6.1% and 10% exhibit long, sloping, or wavy capillary pressure curves. Samples with a porosity exceeding 10% exhibit broad concave capillary pressure curves.

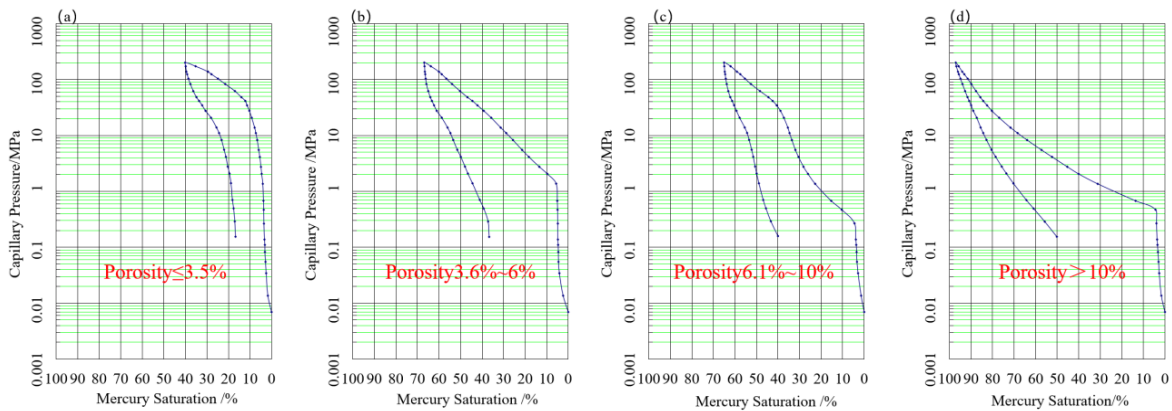


Fig. 14. Morphology of mercury pressure curves grouped by porosity ranges with different porosities in tight sandstone reservoirs of the study area. (a) Porosity $\leq 3.5\%$; (b) Porosity 3.6%-6%; (c) Porosity 6.1%-10%; (d) Porosity $> 10\%$

Classification Criteria for Tight Reservoirs

In summary, analysis of key parameters affecting tight sandstone reservoir properties led to the establishment of a classification system for the coal-bearing strata of the Taihei Sag, Turpan-Hami Basin, using 20 evaluation indicators (Table 1). Reservoirs in the study area are categorized into four classes as follows.

Class I Reservoirs represent the highest reservoir storage and flow capacity in the study area and are primarily composed of sedimentary facies from subaqueous distributary channels at the front margin and plain distributary channels. Diagenesis involves weak compaction and substantial dissolution. Dissolution and primary pores are developed. Capillary pressure curves exhibit a broad concave profile with a median radius exceeding

0.1 μm . Average throat radius surpasses 0.4 μm . Displacement pressure is below 0.7 MPa. Maximum mercury saturation exceeds 80%. Reservoir porosity is $> 10\%$. Permeability typically exceeds 0.5 mD.

Class II Reservoirs represent reservoirs with poor storage and flow capacity in the study area. Primary sedimentary microfacies include subaqueous distributary channels at the front and plain distributary channels, dominated by gravelly medium to coarse-grained sandstones. Diagenesis involves strong compaction (burial and compression) with weak dissolution. Features include solubility, porosity, and microporosity-fracture porosity types. Capillary pressure curves exhibit long-slope or wavy patterns. Median pore radius ranges from 0.01 to 0.1 μm , with average throat radii between 0.1 and 0.4 μm . Displacement pressure spans 0.25 to 1.4 MPa, and maximum mercury saturation ranges from 57% to 83%. Reservoir porosity ranges from 6% to 10%, with permeability distributed between 0.1 and 1 mD. Based on microporous characteristics and clay mineral content, Type II reservoirs are subdivided into Type II₁ and Type II₂: Type II₁ exhibits 70–80% nanoscale porosity, while Type II₂ contains 80–95% nanoscale porosity. Kaolinite and chlorite content in Type II₁ ranges from 4% to 6%, while Type II₂ contains 6% to 8%.

Class III Reservoirs represent poor-quality reservoirs with limited storage and flow capacity in the study area, primarily located at the distal front of plain distributary channels. They consist mainly of gravelly medium sandstone, characterized by strong compaction (burial) and weak dissolution during diagenesis. Tight-type porosity is developed. Capillary pressure curves exhibit wavy or short-slope characteristics. Median pore radius ranges from 0.005 to 0.01 μm . Average throat radius spans 0.05 to 0.25 μm . Displacement pressure lies between 0.4 and 1.4 MPa. Maximum mercury saturation reaches 50% to 70%. Reservoir porosity ranges from 3.5% to 6%, with permeability primarily concentrated between 0.05 and 0.5 mD.

Class IV Reservoirs in the study area have extremely poor storage and flow capacity. These reservoirs are predominantly distributed in foredeeps and shallow lakes. Their capillary pressure curves exhibit a narrow upward-rising profile, with a median radius less than 0.01 μm and an average throat radius less than 0.05 μm . Displacement pressure exceeds 1.4 MPa, and maximum mercury saturation remains below 50%. Reservoir porosity is less than 3.5%, and permeability is generally below 0.2 mD.

Table 1. Valuation criteria for classification of sandstone reservoirs in the coal formations of the Taihei Sag in the Turpan-Hami Basin

Classification Parameters	Reservoir Classification				
	Class I (Excellent)	Class II (Good)		Class III (Moderate)	Class IV (Poor)
		Type II ₁	Type II ₂		
Petrology and Sedimentology Characteristics	Rock Type	Predominantly clastic sandstone	Predominantly clastic sandstone, with feldspar clastic sandstone being secondary.	Predominantly clastic sandstone	Predominantly clastic sandstone
	Sand Body Thickness/m	>40	20-40	10-20	< 10
	Sandstone Grain Size	Coarse sandstone	Gravelly medium sandstone-coarse sandstone	Gravelly medium sandstone	Gravelly medium sandstone
	Sedimentary Microfacies	Frontal underwater diversion channel, Plain diversion channel	Frontal underwater diversion channel, plain diversion channel	Distal end of plain branch channels' front edge	Frontal delta, shallow lakes
	Porosity[%]	> 10	10-6	6-3.5	< 3.5
	Permeability $\times 10^{-3} [\mu\text{m}^2]$	> 0.5	0.1-1	0.05-0.5	< 0.2
Physical Properties	Cement content/%	< 10	4.5-12.5	4-18.5	> 15
	Kaolinite and chlorite content[%]	< 4	4-6	6-8	—
Nuclear magnetic resonance parameters	Movable Fluid Saturation[%]	> 60	55-63	45-55	< 45
	Bound water saturation[%]	< 40	37-45	45-55	> 55
Diagenetic Facies Characteristics	Compaction Strength	Weak compaction	Strong compaction (burial, compression)	Forced Burial (Entombment)	—
	Dissolution Resistance	Strong dissolution	Weak dissolution	Weak dissolution	—
	Microfracture Development	Highly developed	Well-developed	Underdeveloped	Underdeveloped
Pore Structure	Nanoscale Pore Percentage[%]	< 70	70-80	80-95	—
	Average Throat Radius [μm]	> 0.4	0.1-0.4	0.05-0.25	< 0.05
	Displacement	< 0.7	0.25-1.4	0.4-1.4	> 1.4

Pressure[MPa]				
Maximum Mercury Saturation[%]	> 80	57-83	50-70	< 50
Median Radius[μm]	> 0.1	0.01-0.1	0.005-0.01	< 0.01
Capillary Pressure Curve Characteristics	Wider concave type	Long slash type or wavy type	Wave-type or short diagonal-line-type	Narrow upward bulge type
Pore Types	Melting holes - Primary pore patterns	Dissolution-hole type, micro-pore-fracture type	Compact type	—
Reservoir Evaluation	Better	Poor	Bad	Extremely poor
Reservoir Evaluation	Better	Poor	Bad	Extremely poor

Conclusions

(1) The tight sandstones in the study area are mainly lithic sandstones and feldspathic lithic sandstones, composed primarily of clastic grains. These grains are poorly sorted and weakly rounded, with grain contacts dominated by linear arrangements. Reservoir properties are suboptimal, characterized by low porosity and permeability. Pore types are primarily secondary. Compaction is strong within the study area, with close particle contacts. Cementation and alteration are widespread, while dissolution is generally weak.

(2) The porosity of samples in the study area exhibits a strong correlation with sandstone grain size. Compaction exerts the most destructive effect on reservoir properties, cementation has a dual impact, while dissolution improves reservoir properties. Cementation, bound water saturation, and displacement pressure are inversely proportional to porosity with strong correlations. Permeability, median radius, average throat radius, and maximum mercury saturation are positively correlated with porosity, exhibiting strong relationships. Mercury compression curve profiles can be categorized into four types based on distinct porosity ranges.

(3) Based on 20 evaluation indicators, the reservoir in the study area is classified into four categories using porosity thresholds of 10%, 6%, and 3.5%: Class I (excellent) exhibits well-developed dissolution pores-primary pores with large throat radii, displacement pressure of < 0.7 MPa, permeability of > 0.5 mD, and optimal flow characteristics. Class II (good) contains dissolution pores/microporous-fractured type, subdivided into II₁, II₂, with permeability ranging from 0.1 to 1 mD. Class III (moderate) represents tight porosity with poor flow characteristics and permeability between 0.05 and 0.5 mD. Class IV (poor) exhibits extremely poor flow, with a permeability of < 0.2 mD.

References

Ajdukiewicz, J. M., & Larese, R. E. (2012). How clay grain coats inhibit quartz cement and preserve porosity in deeply buried sandstones: Observations and experiments. *AAPG bulletin*, 96(11), 2091-2119. <https://doi.org/10.1306/02211211075>.

Ban S. Y. (2022). Origin of high-quality reservoirs of the lower part of Xishanyao Formation in Taihei Sag, Turpan-Hami Basin (Master's thesis, Lanzhou University). <https://doi.org/10.27204/d.cnki.g1zhu.2022.002361>.

Chen, X., Qu, X. Y., Qiu, L. W., & Zhang, L. Q. (2016). Physical Property of the Upper Paleozoic Tight Sandstone Reservoir and Its Main Controlling Factors during Diagenesis of Well D18 in Daniudi Gas Field. *Acta Sedimentologica Sinica*, 2016, 34(02): 364-374. <https://doi.org/10.14027/j.cnki.cjxb.2016.02.015>.

Cheng J. T. (2021). Reservoir Characteristics of Wutonggou Formation in Permian, Taipei Sag, Turpan-Hami Basin (Master's thesis, China University of Petroleum, Beijing). <https://doi.org/10.27643/d.cnki.gsybu.2021.000298>.

Dai, J. X., Dong, D. Z., Ni, Y. Y., Gong, D. Y., Huang, S. P., Hong, F., Zhang, Y. L., Liu, Q. Y., Wu, X. Q., & Feng, Z. Q. (2024). Distribution patterns of tight sandstone gas and shale gas. *Petroleum Exploration and Development*, 51(04): 667-678. <https://doi.org/10.11698/PED.20240377>.

Dong S. X. (2023). Analysis of the Sources and Origin of Oil and Gas in the Shuixigou Group, Taihei Sag, Turpan-Hami Basin (Master's thesis, Northeast Petroleum University). <https://doi.org/10.26995/d.cnki.gdqsc.2023.000475>.

Guo Q. Q. (2023). Secondary pore development pattern and formation mechanism of He 8 Member in Daning-Jixian area of Ordos Basin, China (Master's thesis, Xi'an Shiyou University). <https://doi.org/10.27400/d.cnki.gxasc.2023.000542>.

Hao, A. S., Li, J., Guo, J. Y., Ran, Q. G., Zhang, H., Qi, X. N., Wu, H., Jia, X. L., Huang, D. F., Chen, X., Kang, J. L., & Shi, Y. J. (2020). Development characteristics and genesis of secondary high porosity zones in deep clastic reservoirs: A case study of the Lower Jurassic in the Taibei Sag of the Tuha Basin. *Natural Gas Industry*, 40(11): 50-59. <https://doi.org/CNKI:SUN:TRQG.0.2020-11-009>.

Hao, A. S., Wu, H., Ran, Q. G., Li, J., Guo, J. Y., Ban, S. Y., Qi, X. N., Chen, X., Tao, H. F., & Jia, X. L. (2021). Provenance and depositional systems of the second member of Lower Jurassic Sangonghe formation in Taibei sag. Turpan-Hami Basin, China. *Journal of China University of Mining and Technology*, 50(05): 893-908. <https://doi.org/10.13247/j.cnki.jcumt.001268>.

Hao, W., Sun, X. X., Lian, J. W., Han, Y. T., Zhang, J. L., Li, Z., Cheng, C. H., Yuan, Y. J., & Sun, L. P. (2025). Prediction of sweet spots in the high-water-content tight sandstone reservoirs of Jurassic Sangonghe Formation in the Tuha Basin. *Natural Gas Industry*, 45(02): 63-72. <https://doi.org/CNKI:SUN:TRQG.0.2025-02-006>.

He, H. Q., Liang, S. J., Guo, X. J., Luo, Q. S., Wang, J. F., Chen, X., Yang, F., Xiao, D. S., & Zhang, H. (2022). New discoveries and exploration prospects of Middle and Lower Jurassic lithologic reservoirs in depression area of Turpan-Hami Basin. *Natural Gas Geoscience*, 33(7): 1025-1035. <https://doi.org/10.11764/j.issn.1672-1926.2022.02.004>.

Jia, A. L., Wei, Y. S., Guo, Z., Wang, G. T., Meng, D. W., & Huang, S. Q. (2022). Development status and prospect of tight sandstone gas in China. *Natural Gas Industry*, 42(01): 83-92. <https://doi.org/CNKI:SUN:TRQG.0.2022-01-008>.

Li, G., Li, C., Zhang, B., Zhang, L., Liang, Z., & Chen, Q. (2024). Characterization of reservoir quality in tight sandstones from the Benxi Formation, eastern Ordos Basin, China. *Frontiers in Earth Science*, 12, 1377738. <https://doi.org/10.3389/feart.2024.1377738>.

Li, G. X., & Zhu, R. K. (2020). Progress, challenges and key issues of unconventional oil and gas development of CNPC. *China Petroleum Exploration*, 25(02): 1-13. <https://doi.org/CNKI:SUN:KTSY.0.2020-02-001>.

Li, G. Y., Pang, X. Y., Zhang, Y., Lai, F. Q., He, J. C., & Liu, J. (2015). Physical Characteristics and Controlling Factors of Tight Sandstone in Turpan-Hami Basin—Sangonghe Formation, Western Shengbei Sag. *Xinjiang Geology*, 33(04): 515-519.

Li, J. Z., Yang, F., Xiao, D. S., Chen, X., Wu, C., Zhang, H., Yu, H. Y., Jia, X. L., & Chen, G. (2025). Analysis of hydrocarbon accumulation differences and exploration Directions in the Taibei Sag, Turpan-Hami Basin. *Natural Gas Geoscience*, 1-14. <https://doi.org/10.11764/j.issn.1672-1926.2025.04.012>.

Liu, X., Zhong, J. H., Sun, Y. K., Wang, J. S., Wei, T., & Qu, J. L. (2014). Analysis of the reservoir performance influencing factors of the tight sandstone gas accumulations in the Shuixigou Group, Turpan-hami Basin. *Journal of Northwest University (Natural Science Edition)*, 44(03): 451-460. <https://doi.org/10.16152/j.cnki.xdbzr.2014.03.017>.

Liu, X. J., Ma, Z. J., Han, D., Wang, H. Y., Ma, L. T., & Ge, D. S. (2018). Research on the main factors of high quality tight sandstone reservoir in Linxing block, Ordos Basin. *Natural Gas Geoscience*, 29(04): 481-490. <https://doi.org/CNKI:SUN:TDKX.0.2018-04-004>.

Ma J. (2024). Evaluation of exploration potential for coal-measure tight sandstone gas in Shuixigou Group of Shisanjianfang area, Turpan-Hami Basin. *Journal of Shandong Institute of Petroleum and Chemical Technology*, 38(02): 1-11. <https://doi.org/CNKI:SUN:SLYS.0.2024-02-001>.

Ni, L. T., Zhong, J. H., Wang, G. L., Sun, N. L., Liu, X., Hao, B., Sun, Y. K., Wang, J. S., Yang, B., & Qu, J. L. (2022). A new gas accumulation theory of tight sandstone gas accumulation in Turpan-Hami Basin—proximal-generation and proximal storage type and self-generation and self-storage type. *Coal Science and Technology*, 50(03): 176-186. <https://doi.org/10.13199/j.cnki.cst.2019-0691>.

Ni, Y. Y., Liao, F. R., Gong, D. Y., Jiao, L. X., Gao, J. L., & Yao, L. M. (2019). Stable carbon and hydrogen isotopic characteristics of natural gas from Taibei Sag, Turpan-Hami Basin, NW China[J]. *Petroleum Exploration and Development*, 46(3): 531-542. [https://doi.org/10.1016/S1876-3804\(19\)60033-9](https://doi.org/10.1016/S1876-3804(19)60033-9).

Si, X. Q., Cao, Q. B., Ji, W. H., Chen, C. X., Wang, X., & Zhi, F. Q. (2014). Characteristics and Influence Factors of Tight sandstone Reservoirs of Shuixigou Group in Taibei Sag, Turpan-Hami Basin. *Journal of Mineralogy and Petrology*, 34(4): 93-101. <https://doi.org/10.19719/j.cnki.1001-6872.2014.04.011>.

Tang, W. B., Lei, T., Xu, S. L., & Chen, A. Q. (2015). The Study of Kalaza Formation Sand Reservoir Characteristics and Diagenesis in Shengbei-Honglian Area of Tuha Basin. *Science Technology and Engineering*, 15(18): 40-49. <https://doi.org/CNKI:SUN:KXJS.0.2015-18-009>.

Wang, J., Ye, F. W., Zhang, C., & Xi, Z. D. (2023). Factors That Control the Reservoir Quality of the Carboniferous-Permian Tight Sandstones in the Shilounan Block, Ordos Basin. *Processes*, 11(8), 2279. <https://doi.org/10.3390/pr11082279>.

Wang, W. M., Lu, S. F., Li, J., Tian, W. C., Zhou, N. W., & Huang, W. B. (2016). Analyses of micro pore structural characteristics of tight sandstone reservoirs: A case study in Turpan-Hami Basin, northwestern China. *Natural Gas Geoscience*, 27(10): 1828-1836. <https://doi.org/CNKI:SUN:TDKX.0.2016-10-008>.

Wang, W. M., Zhao, X., Duan, S. Q., Wang, Y., Wang, G. L., Yan, X., & Tian, W. C. (2014). Key parameter selection for tight gas resource potential: a case from Turfan-Hami Basin. *Oil and Gas Geology*, 35(02): 258-26. <https://doi.org/CNKI:SUN:SYYT.0.2014-02-015>.

Xiao, D. S., Zhang, H., Cheng, Y., Liu, J. T., Gou, H. G., You, F., Zhang, Y. T., & Guo, S. (2024). Study on the Characteristics and Main Controlling Factors of Tight Sandstone Reservoirs of Sangonghe Formation in the Shengbei SubSag of the Tuha Basin. *Journal of Jilin University(Earth Science Edition)*.1-15. <https://doi.org/10.13278/j.cnki.jjuese.20240316>.

Xu Y Q. (2019). Research on characteristics of microscopic pore throat and classified evaluation of Chang7 tight sandstone reservoir in Longdong area, Ordos Basin. (Doctoral dissertation, Northwest University). Ph.D. <https://doi.org/10.27405/d.cnki.gxbdu.2019.000197>.

Yang G Q. (2021). Research on Genetic Mechanism of High-quality Tight Sandstone Reservoirs of Upper Paleozoic in Linxing-Shenfu Area (Doctoral dissertation, China University of Geosciences, Beijing). <https://doi.org/10.27493/d.cnki.gzdzy.2021.000090>.

Yu, H. Y., Xiao, D. S., & Wang, B. (2024). Diagenesis and diagenetic facies of deep and ultra deep tight sandstone in Turpan-Hami Basin: a case study of the second Member of Sangonghe Formation in the J7 well area, Qiudong Subsag. *Fault-Block Oil & Gas Field*, 31(03): 369-378. <https://doi.org/10.6056/dkyqt202403001>.

Zhang Q. H. (2020). Study on Distribution Characteristics of Upper Triassic Reservoirs in Toksun Depression, Tuha Basin (Master's thesis, China University of Petroleum (East China)). <https://doi.org/10.27644/d.cnki.gsydu.2020.000770>.

Zhang, C., Li, X. P., Zhong, J. H., & Zhang, T. F. (2011). Properties and the Main Controlling Factors of Compact Sandstone Reservoirs in Lower Jurassic Series of Baka Oilfield in Tuha Basin. *Journal of Shandong University of Science and Technology*, 30(06): 65-72. <https://doi.org/10.16452/j.cnki.sdkjzk.2011.06.008>.

Zhang, S., Wang, J., Liu, C., Bai, J., Peng, H., Huang, H., & Guan, Y. (2019). Detritalzircon U-Pb geochronology of the Permian strata in the Turpan-Hami Basin in North Xinjiang, NW China: Depositional age, provenance, and tectonic implications. *Geological Journal*, 54(2), 1064-1080. <https://doi.org/10.1002/gj.3374>.

Zhi, D. M., Li, J. Z., Yang, F., Chen, X., Wu, C., Wang, B., Zhang, H., Hu, J., & Jin, J. K. (2024). Whole Petroleum System in Jurassic Coal Measures of Taihei Sag in Tuha Basin, NW China. *Petroleum Exploration and Development Online*, 51(3): 519-534. [https://doi.org/10.1016/S1876-3804\(24\)60485-4](https://doi.org/10.1016/S1876-3804(24)60485-4).

Zhou D. (2023). Research on the genetic mechanism of tight sandstone reservoirs of Middle Jurassic Shaximiao Formation in the area between the central and western Sichuan Basin (Master's thesis, Chengdu University of Technology). <https://doi.org/10.26986/d.cnki.gedlc.2023.001112>.

Zhou Y. (2020). Formation and Distribution of the High-quality Reservoirs of Deep Jurassic in Taihei Sag, Tuha Basin. (Master's thesis, China University of Petroleum, Beijing). <https://doi.org/10.27643/d.cnki.gsybu.2020.001179>.

Zhou, G., Cheng, T., Li, J., Chen, A. Q., Li, F. X., Xu, H., & Xu, S. L. (2023). Diagenesis and Pore Evolution of Tight Reservoirs of Sanjianfang Formation in Shengbei Subsag. *Xinjiang Petroleum Geology*, 44(03): 289-298. <https://doi.org/CNKI:SUN:XJSD.0.2023-03-004>.

Zhou, N. W., Lu, S. F., Wang, M., Huang, W. B., Xiao, D. S., Jiao, C. X., Wang, J. M., Tian, W. C., Zhou, L., Chen, F. W., Liu, W., & Wang, Z. X. (2021). Limits and grading evaluation criteria of tight oil reservoirs in typical continental basins of China. *Petroleum Exploration and Development*, 48(05): 939-949. [https://doi.org/10.1016/S1876-3804\(21\)60093-9](https://doi.org/10.1016/S1876-3804(21)60093-9).